

Phase transitions in $\text{Co}_{78}\text{Si}_9\text{B}_{13}$ and $\text{Fe}_{78}\text{Si}_9\text{B}_{13}$ metallic glasses induced by isochronal annealing

E. JAKUBCZYK*

Institute of Physics, Jan Długosz University, al. Armii Krajowej 13/15, 42-201 Częstochowa, Poland

The crystallization process of $\text{Co}_{78}\text{Si}_9\text{B}_{13}$ and $\text{Fe}_{78}\text{Si}_9\text{B}_{13}$ metallic glasses was stimulated by isochronal annealing at various temperatures (573–823 K). By the DSC, X-ray diffraction, Hall and electrical resistivity measurements it was found that the crystallization proceeds through two main stages. At the first stage, α -Co and α -Fe phases are formed and at the second stage Co_2B and Fe_2B phases are crystallized. During the crystallization, the ferromagnetic ordering of both alloys is still conserved. $\text{Fe}_{78}\text{Si}_9\text{B}_{13}$ alloy has a much wider range of structural stability. The activation energy determined from DSC measurements and the total energy of the created phases obtained by quantum chemistry method confirmed the sequence and the type of the created phases. The creation of crystalline phases from the amorphous matrix was related to a distinct decrease of the electrical and Hall resistivities and the spontaneous Hall coefficient.

Key words: *metallic glass; crystallization; phase transition; activation energy; Hall effect*

1. Introduction

Rapid solidification from liquid state leads to the formation of a metastable amorphous structure. Metallic glasses are obtained in this way and they evolve through changes of the chemical and topological short-range ordering (CSRO and TSRO) and then changes of medium range ordering (MRO) to a polycrystalline state [1, 2]. The initiation and the kinetics of the crystallization process depend on their anisotropic microstructure and fluctuations of defect density. The transformation of the amorphous to the crystalline state can occur by the following typical processes: polymorphous, eutectoid, primary and peritectoid crystallization [3]. The type of transformation depends mainly on the alloy composition. The investigation of phase transitions in metallic glasses is important from both scientific and application points of view. This paper concentrates on the analysis of the influence of composition on the struc-

*Corresponding author, e-mail: e.jakubczyk@ajd.czyst.pl

ture relaxation caused by isochronal annealing. For comparison, the most distinctive glasses from the $\text{Fe}_{78-x}\text{Co}_x\text{Si}_9\text{B}_{13}$ family, i.e. $\text{Co}_{78}\text{Si}_9\text{B}_{13}$ and $\text{Fe}_{78}\text{Si}_9\text{B}_{13}$ were chosen. The structural changes coincide with the changes of physical properties, and the latter ones are especially significant when a phase transition occurs. Standard methods have been applied to study the phase transitions, i.e. the DSC (differential scanning calorimetry), X-ray diffraction, electrical resistivity as well as the investigation of the Hall effect. The combination of methods makes it possible to determine the order of phase transition and also the type scattering of charge carriers [4–6].

2. Experimental

Ribbons of $\text{Co}_{78}\text{Si}_9\text{B}_{13}$ and $\text{Fe}_{78}\text{Si}_9\text{B}_{13}$ metallic glasses were prepared by the roller quenching method. DSC measurements were carried out using a STA-409 NETZSCH apparatus under an argon stream at heating rates of 5, 10, 15 and 20 K/min. Measurements of the electrical and Hall resistivities and X-ray diffraction were done at room temperatures for the as-received as well as isochronally (4 h) annealed samples at various temperatures (573–823 K) in an inert argon atmosphere. The X-ray studies were performed using a DRON-2.0 diffractometer with MoK_α radiation. The Hall voltage was measured by the constant current method at a constant magnetic field [7]. The electrical resistivity was also measured in the dc regime. The quantum-chemical calculations of the total energy of the created phases were done using a semi-empirical method of the HyperChem 6.0 program [8, 9].

3. Results and discussion

The thermal stability and kinetics of non-isothermal crystallization of $\text{Co}_{78}\text{Si}_9\text{B}_{13}$ and $\text{Fe}_{78}\text{Si}_9\text{B}_{13}$ metallic glasses were investigated by the DSC measurements. The measurements of the crystallization process were carried out for alloys at the heating rates of 5, 10, 15 and 20 K/min.

Figures 1a and 2a show the DSC curves of both alloys taken at various heating rates. It is clearly seen that all the DSC curves display two exothermic peaks indicating that the transformation of the amorphous to the polycrystalline state proceeds through two main stages. The temperatures corresponding to both peaks of both alloys increase with the increase of the heating rate. In the case of $\text{Co}_{78}\text{Si}_9\text{B}_{13}$, the exothermic peaks in DSC curves are widely separated, while those of $\text{Fe}_{78}\text{Si}_9\text{B}_{13}$ are closely situated. The temperature for the first peak for $\text{Co}_{78}\text{Si}_9\text{B}_{13}$ alloy is lower than that for the $\text{Fe}_{78}\text{Si}_9\text{B}_{13}$ alloy. Based on the Kissinger equation, the activation energy E_a for crystallization of phases can be estimated as follows [10–12]:

$$\frac{d\left(\ln\frac{\nu}{T_p^2}\right)}{d\left(\frac{1}{T_p}\right)} = -\frac{E_a}{R} \quad (1)$$

where ν denotes the heating rate, T_p – peak temperature and R is the gas constant.

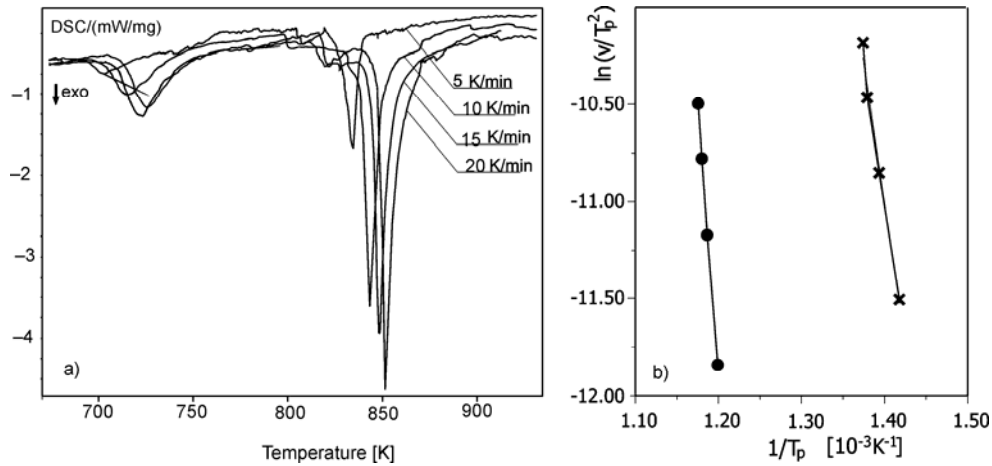


Fig. 1. Dependences for $\text{Co}_{78}\text{Si}_9\text{B}_{13}$ metallic glass: a) DSC curves at various heating rates, b) relationship between $\ln(\nu/T_p^2)$ and $1/T_p$ for both stages of crystallization (• – first stage, × – second stage)

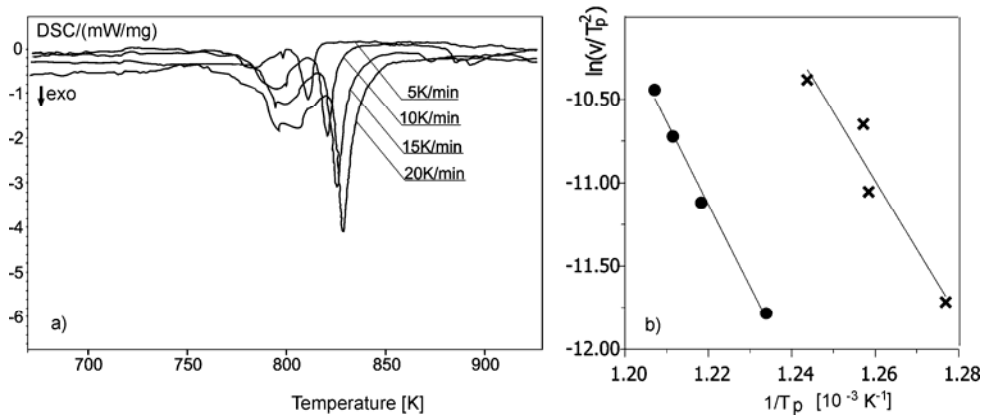


Fig. 2. Dependences for $\text{Fe}_{78}\text{Si}_9\text{B}_{13}$ metallic glass: a) DSC curves at various heating rates; b) relationship between $\ln(\nu/T_p^2)$ and $1/T_p$ for both stages of crystallization (• – first stage, × – second stage)

The plots of $\ln(\nu/T_p^2)$ vs. $1/T_p$ for both alloys yield straight lines with the slopes equal to $-E_a/R$ (Figs. 1b, 2b).

The values of the activation energy for the first and the second stage of crystallization for $\text{Co}_{78}\text{Si}_9\text{B}_{13}$ and $\text{Fe}_{78}\text{Si}_9\text{B}_{13}$ metallic glasses are given in Table 1. Thermal stimulation of the crystallization process for the first stage of the crystallization requires higher activation energy for the $\text{Fe}_{78}\text{Si}_9\text{B}_{13}$ alloy in comparison with $\text{Co}_{78}\text{Si}_9\text{B}_{13}$. The other results presented in this paper confirm occurring of the structural changes in the $\text{Fe}_{78}\text{Si}_9\text{B}_{13}$ metallic glass after annealing at higher temperatures.

Table 1. The activation energies [kJ/mol] for the first (E_{a1}) and the second (E_{a2}) stage of crystallization for $\text{Co}_{78}\text{Si}_9\text{B}_{13}$ and $\text{Fe}_{78}\text{Si}_9\text{B}_{13}$ metallic glasses

$\text{Co}_{78}\text{Si}_9\text{B}_{13}$		$\text{Fe}_{78}\text{Si}_9\text{B}_{13}$	
E_{a1}	E_{a2}	E_{a1}	E_{a2}
241	472	341	410

Figures 3 and 4 show the results of the measurement of the Hall resistivity ρ_H as a function of the external magnetic field B_0 in the as-received samples and in the samples annealed isochronally at various temperatures. With the increase of the annealing temperature ρ_H decreases. For the $\text{Co}_{78}\text{Si}_9\text{B}_{13}$ alloy the first decrease of the slope of the initial part of the dependence $\rho_H = f(B_0)$, as well as the decrease of the magnitude of the next part (slowly increasing) of this curve occurs for the samples annealed at 623 K. The next distinct steps are observed for the samples annealed at 673 K and 773 K.

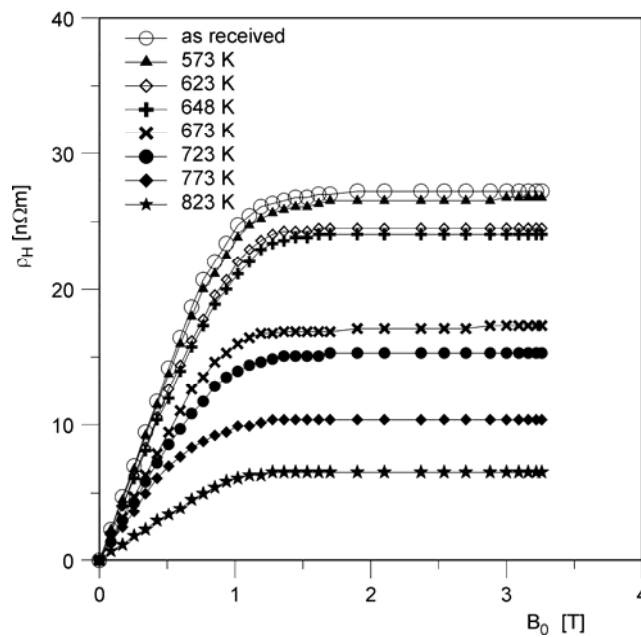


Fig. 3. The Hall resistivity ρ_H as a function of the applied magnetic induction B_0 for the samples of the $\text{Co}_{78}\text{Si}_9\text{B}_{13}$ alloy annealed at various temperatures

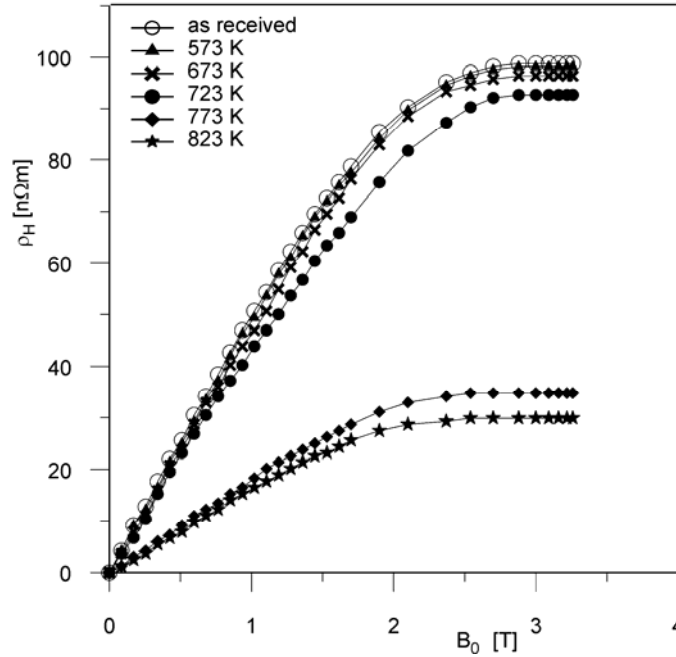


Fig. 4. The Hall resistivity ρ_H as a function of the applied magnetic induction B_0 for the samples of the $\text{Fe}_{78}\text{Si}_9\text{B}_{13}$ alloy annealed at various temperatures

For the $\text{Fe}_{78}\text{Si}_9\text{B}_{13}$ alloy the abrupt decrease of curves $\rho_H = f(B_0)$ occurs for the samples annealed at 723 K and 773 K. The investigated alloys are the ferromagnetic materials and therefore the Hall resistivity is [4–6, 13]:

$$\rho_H = R_0 B_0 + \mu_0 R_s M \quad (2)$$

where R_0 and R_s are the ordinary and spontaneous Hall coefficients, respectively, and M is the magnetization of the sample. Each curve from Figs. 3 and 4 is typical of ferromagnetic substances. This demonstrates that during the crystallization process the macroscopic ferromagnetic ordering of both alloys is conserved. The first term of Eq. (2) is the ordinary Hall resistivity ($\rho_{H_0} \propto B_0$). It is related to the Lorentz force acting on the current carriers and corresponds to the slowly growing part of the $\rho_H = f(B_0)$ curve above the magnetization saturation. The second term is the spontaneous Hall effect ($\rho_{H_s} \propto M$) and is represented by the initial part of the $\rho_H = f(B_0)$ curve. The ρ_{H_s} is connected with a ferromagnetic state and determined by the following mechanisms: spin-orbit interaction, skew scattering and side jump [4, 5]. These mechanisms decrease the mean free path of carriers. For the initial part of the $\rho_H = f(B_0)$ curves the spontaneous Hall coefficient R_s was calculated using the linear regression

$$R_s = \left(\frac{\partial \rho_H}{\partial B_0} \right)_{B_0 \rightarrow 0}$$

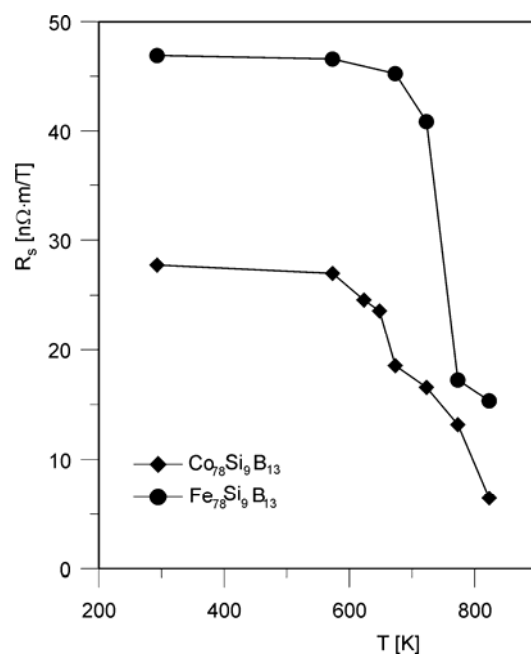


Fig. 5. The spontaneous Hall coefficient R_s , as a function of annealing temperature T for the samples $\text{Co}_{78}\text{Si}_9\text{B}_{13}$ and $\text{Fe}_{78}\text{Si}_9\text{B}_{13}$ alloys

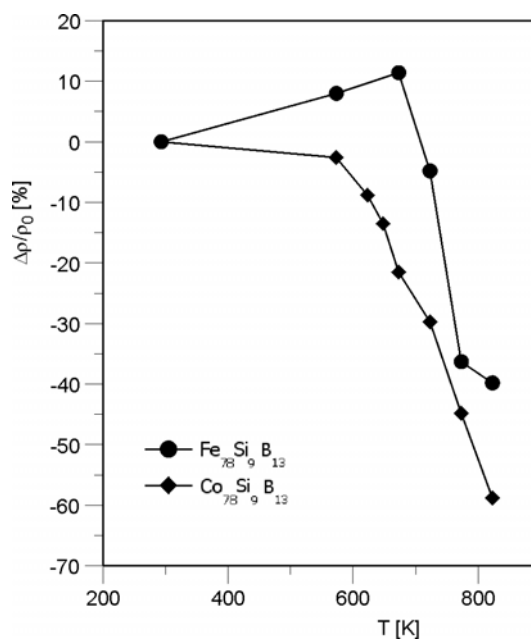


Fig. 6. The relative electrical resistivity $\Delta\rho/\rho_0$ as a function of annealing temperature T for the samples of $\text{Co}_{78}\text{Si}_9\text{B}_{13}$ and $\text{Fe}_{78}\text{Si}_9\text{B}_{13}$ alloys

Figure 5 presents the dependence of R_s on the annealing temperature T for both alloys. Figure 6 shows relative changes of the electrical resistivity ρ (related to the resistivity of the as-received state ρ_0) vs. the annealing temperature. For the $\text{Fe}_{78}\text{Si}_9\text{B}_{13}$ alloy, an increase of $\Delta\rho/\rho_0$ value in the initial step of annealing is observed, connected with the structural changes of TSRO type. The decrease of the electrical resistivity during the crystallization is due to the increase of the free path of the carriers in ordered structure in medium and long range.

According to Berger and Bergmann, the spontaneous Hall coefficient R_s is described by the dependence [4–6]:

$$R_s = a\rho + b\rho^2 \quad (3)$$

where a and b are constants roughly independent of temperature and ρ is the resistivity.

The first term of Eq. (3) is responsible for the classical asymmetric scattering of charge carriers and the second term describes the quantum effect and corresponds to the lateral displacement of the charge carrier trajectory at the point of scattering, i.e. the side jump. The dependence of $\lg R_s$ on $\lg \rho$ gives the exponent n in the relation $R_s \propto \rho^n$ and through its value it can be concluded which type of scattering is dominant for the spontaneous Hall effect. Figure 7 shows these dependences for both alloys. The calculated exponents n for $\text{Co}_{78}\text{Si}_9\text{B}_{13}$ and $\text{Fe}_{78}\text{Si}_9\text{B}_{13}$ are 1.58 and 1.91, respectively. The values n indicate that during the crystallization process the charge carriers are mainly scattered by nonclassical mechanism, i.e. side jump.

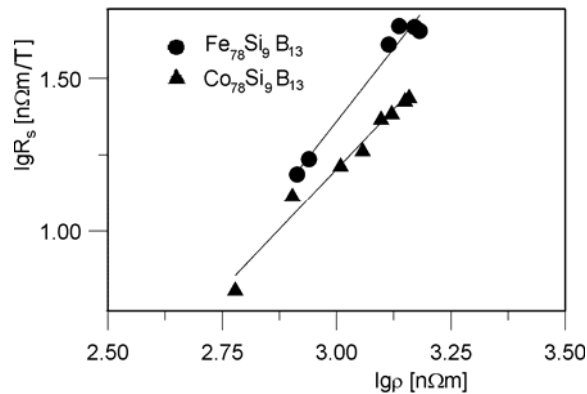


Fig. 7. The dependence of $\lg R_s$ on $\lg \rho$ for $\text{Co}_{78}\text{Si}_9\text{B}_{13}$ and $\text{Fe}_{78}\text{Si}_9\text{B}_{13}$ alloys annealed at various temperatures

To analyse the structural changes and identify the crystalline phases formed from the amorphous matrix, the X-ray diffraction investigations for the as-received as well as annealed samples were performed (Fig. 8.). The results prove that the first stage of the crystallization begins after the annealing of the samples at 648 K and 723 K for the $\text{Co}_{78}\text{Si}_9\text{B}_{13}$ and $\text{Fe}_{78}\text{Si}_9\text{B}_{13}$ alloys, respectively. A qualitative analysis proves that they are the α -Co and α -Fe phases [14]. After annealing at 773 K, the phases Co_2B

and Fe_2B are created. It is possible that the metallic phases include a certain amount of Si [15–17].

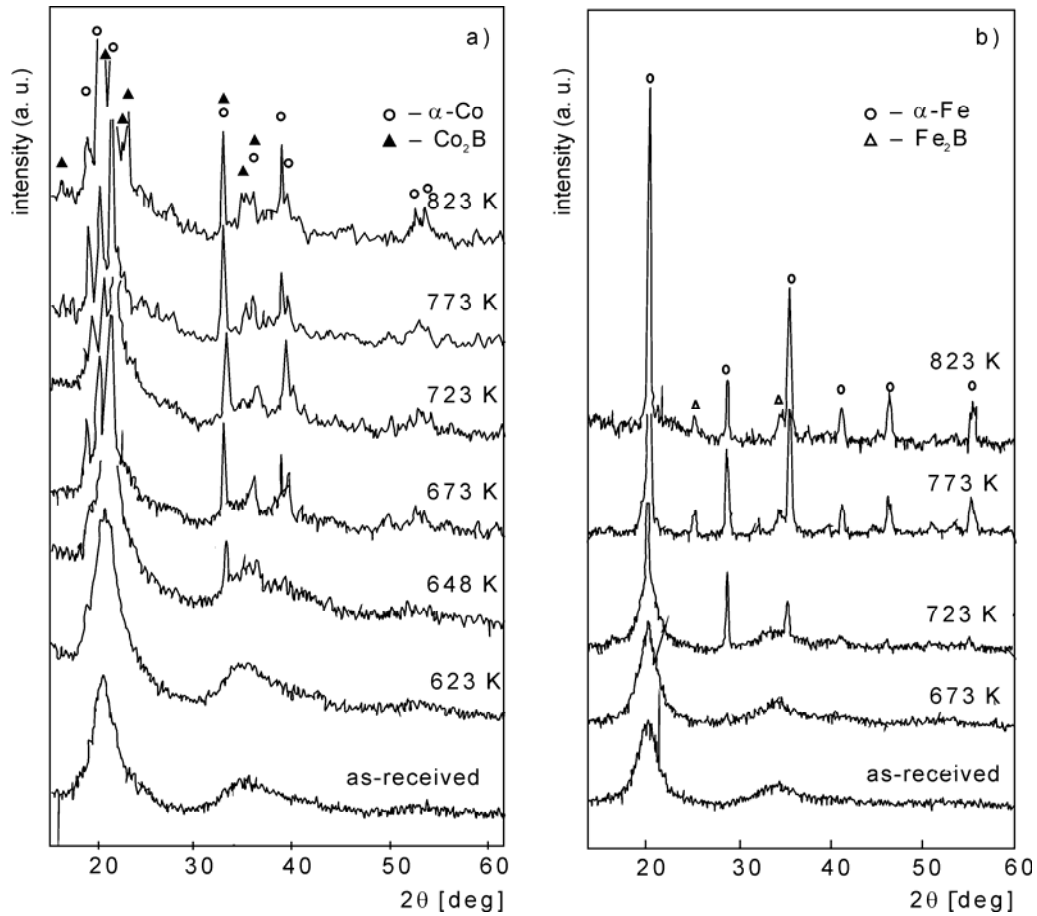


Fig. 8. X-ray diffraction patterns for the samples of alloys: a) $\text{Co}_{78}\text{Si}_9\text{B}_{13}$ and b) $\text{Fe}_{78}\text{Si}_9\text{B}_{13}$

The first stage of crystallization of both alloys occurs as a result of the primary crystallization and the second one as a result of the polymorphous crystallization. The structural changes appear in the measurements of the electrical and Hall resistivities after annealing at temperatures lower than in X-ray diffraction and DSC studies. It demonstrates that the methods involving the electronic transport are more sensitive to structural changes.

To verify the sequence of the created phases determined by the X-ray diffraction, quantum chemical calculations of the total energy of the model clusters were carried out. The value of the total energy of $\alpha\text{-Co}$ clusters ($-22\,8327.7$ kcal/mol) is lower than that of Co_2B clusters ($-16\,1397$ kcal/mol). The obtained energies for $\alpha\text{-Fe}$ ($-16\,3806$ kcal/mol) and Fe_2B ($-11\,9125.9$ kcal/mol) are in an analogous rela-

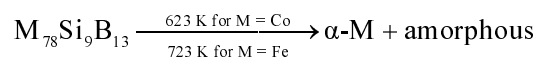
tion. These results prove that in both alloys the metallic phases crystallize first from the amorphous matrix during the annealing because they require less energy in comparison with borides which crystallize at higher temperatures.

The differences between the calculated values of the energy of metallic and boride phases are 66 930.7 kcal/mol and 44 680.1 kcal/mol for $\text{Co}_{78}\text{Si}_9\text{B}_{13}$ and $\text{Fe}_{78}\text{Si}_9\text{B}_{13}$, respectively. The difference between the temperature of crystallization of metallic and boride phases in the alloy with Co is higher than that of the alloy with Fe and it confirms the results of the DSC measurements.

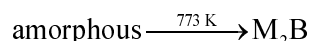
4. Conclusions

The crystallization processes of $\text{Co}_{78}\text{Si}_9\text{B}_{13}$ and $\text{Fe}_{78}\text{Si}_9\text{B}_{13}$ metallic glasses proceed in two stages. At the first stage, α -Co and α -Fe phases crystallize and at the second one, Co_2B and Fe_2B phases are formed during annealing. The most sensitive method of examination of structural changes is the Hall effect. With this method, the following temperatures of the phase transitions of the first order for the first and the second stage were found:

- first stage



- second stage



The $\text{Fe}_{78}\text{Si}_9\text{B}_{13}$ alloy has a wider thermal range of structural stability.

The substitution of Co with Fe drastically increases the Hall resistivity in the as-received state and it is connected with the increase of scattering of charge carriers by Fe atoms. During the crystallization process, the ferromagnetic order of both alloys is conserved. The dominant type of scattering of charge carriers is the side jump effect. The Hall and electrical resistivities decrease abruptly after the crystallization of a suitable phase. The activation energy for both stages of crystallization as well as the total energy for clusters of created phases obtained from DSC measurements and quantum chemistry method prove that at the first stage the metallic phases are created and at the second one the metal borides are formed.

References

- [1] VAN DEN BEUKEL A., RADELAAR S., *Acta Metall.*, 31 (1983), 419.
- [2] VAN DEN BEUKEL A., *Key Engin. Mater.*, 81–83 (1993), 3.
- [3] KOSTER U., *Key Eng. Mater.*, 81–83 (1993), 647.
- [4] BERGER L., BERGMANN G., *The Hall Effect of Ferromagnets*, [in:] C.L. Chien, C.R. Westgate (Eds.), *The Hall Effect and Its Applications*, Plenum Press, New York, 1980, 55.

- [5] MCGUIRE T.R., GAMBINO R.J., O'HANDLEY R.C., *Hall Effect In Amorphous Metals*, [in:] C.L. Chien, C.R. Westgate (Eds.), *The Hall Effect and Its Applications*, Plenum Press, New York, 1980, 137.
- [6] STOBIECKI T., PRZYBYLSKI M., *Phys. Stat. Sol. (b)*, 134 (1986), 131.
- [7] JAKUBCZYK E., *Acta Phys. Polon. A*, 99 (2001), 673.
- [8] *HyperChem™, Release 6.01 for Windows, Molecular Modelling System*, Hypercube, Inc., 2000.
- [9] JAKUBCZYK E., JAKUBCZYK M., *Czech J. Phys.*, 54 (2004), D165.
- [10] KISSINGER H.E., *Anal. Chem.*, 29 (1957), 1702.
- [11] WANG H.R., GAO Y.L., HUI X. D., MIN G.H., CHEN Y., YE Y.F., *J. Alloys Comp.*, 349 (2003), 129.
- [12] SHAPAAN M., LENDVAY J., VARGA L.K., *J. Non-Cryst. Sol.*, 330 (2003), 150.
- [13] HURD C.M., *The Hall Effect in Metals and Alloys*, Plenum Press, New York, 1972.
- [14] VILLARS P., *Pearson's Handbook Desk Edition, Crystallographic Data for Intermetallic Phases*, ASM International, Materials Park, OH 44073, USA, 1997.
- [15] BANERJI N., JOHRI U.C., KULKARNI V.N., SINGRU R.M., *J. Mater. Sci.*, 30 (1995), 417.
- [16] WOLNY J., SMARDZ L., ZAJĄC W., SOLTYS J., DUBOIS J. M., *J. Magn. Magn. Mater.*, 41 (1984), 191.
- [17] JAKUBCZYK E., MANDECKI Z., FILIPECKI J., *J. Non-Cryst. Solids*, 192, 193 (1995), 509.

Received 9 September 2005

Revised 9 November 2005